



Encapsulation of Triazole Derivatives Conjugated with Selenium Nanoparticles onto Nano-Chitosan for Antiproliferative Activity towards Cancer Cells

Ahmed E. Abdelhamid ¹, Ahmed A. Elsayed ², Samira A. Swelam ²,
Abdelmohsen M. Soliman ³, Ahmed M. Khalil ^{2*}



¹Polymers & Pigments Department, National Research Centre, El-Bohouth St., Dokki - 12622, Giza, Egypt

²Photochemistry Department, National Research Centre, 33 El-Bohouth St., Dokki - 12622, Giza, Egypt

³Therapeutic Chemistry Department, National Research Centre, 33 El-Bohouth St., Dokki - 12622, Giza, Egypt

Abstract

Encapsulation of synthesized triazole derivatives in the presence or absence of selenium nanoparticles (SeNPs) into nano-chitosan was directed to be employed in cancer treatment. The synthesized nano-capsules were well characterized using FTIR, TEM, DLS, and TGA. The results indicated that the nanoparticles exhibited a spherical shape with the size range of 50-80 nm as they were conjugated with triazole derivatives inside the capsules. These conjugated selenium nano-capsules showed enhanced thermal stability. The cytotoxicity and in vitro anticancer evaluation of the synthesized triazole derivatives loaded onto nano-chitosan through the samples (**2a**, **2b**, **3a** and **3b**) have been assessed for human colon cancer cell line (HCT116). These samples are conjugated with selenium nanoparticles. The results showed that the in vitro antiproliferative activity of the newly synthesized compounds was significant and may be tested through further in vivo and pharmacokinetic studies.

Keywords: Selenium Nanoparticles; Triazole; Nano-Chitosan; Encapsulation; Anticancer Activity; Colon Cancer; Cell Line (HCT116)

1. Introduction

Cancer is a leading global cause for millions of deaths annually [1]. However, the medical treatment of malignant tumors is not sufficient enough. So, the development of novel agents with reasonable therapeutics is the key topic with much concern [2]. Selenium nanoparticles (SeNPs) are considered to stand out among the most encouraging exploration introduction for oncotherapy [3–5]. Biomedical applications of SeNPs comprise a drug and targeted gene delivery. Moreover, anticancer, antibacterial and anti-inflammatory efficiencies are considered [6–8]. Some heterocyclic azo-based compounds showed reliable results upon been utilized pharmaceutical applications [9]. Targeting the anticancer drugs including tumour-specific cell signalling, cell division, energy metabolism, gene expression, and drug resistance are essential to enhance the efficacy of antitumor drugs with lower toxicity. Heterocyclic compounds are considered as major components in chemical

therapeutics. Thereafter, it is recommended to reduce the use of chemicals as much as possible to synthesize the targeted heterocyclic compounds. Natural sources are preferred to afford biocatalysts for the synthesis reactions [10,11]. Some triazoles; either prepared in the lab or isolated from natural products show many pharmacological properties. They possess antibacterial, anti-cancer and anti-malarial properties [10,12,13]. Nucleosides contribute to different pharmacological and biological applications. They exhibit antiviral, anticancer, and antimicrobial activities [14,15]. In cancer chemotherapy, nanomedicines for administration have become highly relevant since the use of nanoparticulated drug delivery systems has offered several advantages over conventional drug administration [16–18].

Metallic nanoparticles comprising selenium nanoparticles (SeNPs) have roles in biological and medical implications [5,19]. They comprise drug and targeted gene delivery and anticancer activity [20]. They supply many ways to control the release profile

*Corresponding author e-mail akhalil75@yahoo.com

Receive Date: 28 June 2022, Revise Date: 12 July 2022, Accept Date: 24 July 2022, First Publish Date: 24 July 2022

DOI: 10.21608/EJCHEM.2022.147872.6401

©2022 National Information and Documentation Center (NIDOC)

of encapsulated moieties. (SeNPs) can be prepared by many methods including laser ablation, microwave-assisted, chemical reduction, electro-deposition, solvo-thermal and green synthesis. Natural polymers such as chitosan possess advantages over their synthetic counterparts regarding inherent bioactivity. They are able to possess receptor binding ligands to cells with greater susceptibility to degradation due to cellular enzymatic action [21,22]. However, they may have some disadvantages such as a strong immunogenic response and complexities associated with their purification. The biocompatibility and biodegradability of these polymers, accompanied by the ease of chemical modification and blending, allowed them to be essential platforms for the development of an impressive amount of research. This feature is the clearest proof of the potential of this polymer in biomedicine and pharmaceuticals [23–25]. Chitosan showed promising results in the delivery of anticancer chemotherapeutics towards targeted tumor cells. Nano-chitosan loaded with therapeutics appears to be more stable, permeable, and bioactive [26]. The main objective of this work is to synthesize novel heterocyclic compounds of triazole moieties using ecofriendly methods to act as selective anticancer agents. In this approach, we are focusing on employing sono-synthesized selenium loaded onto nano-chitosan to contribute in this application.

2. Materials and Methods

2.1. Materials

Low molecular weight chitosan (Mwt. <100 kDa) was provided from Bio Basic Inc. (Canada). Sodium tripolyphosphate (TPP), selenous acid and dimethyl sulfoxide (DMSO) were purchased from Sigma Aldrich, USA. Acetic acid was of analytical grade and provided from El-Nasr Company - Egypt.

2.2. Synthesis of triazole encapsulated chitosan

All the compounds are synthesized according to the previous research article by Khattab R. et. al. (2021) [5].

Synthesis of compounds 2a,b & 3a,b

An equimolar mixture of compound **1a,b** (10 mmol) and respective monosaccharides (Glucose and Xylose) or 2,3,4-trimethoxybenzaldehyde (10 mmol) was dissolved in ethanol (10 ml) and certain amounts of acetic acid. The reaction mixture was refluxed for eight hours. The reaction mixture was allowed to cool at room temperature the formed solid was filtered off and washed with cold ethanol. The solid was recrystallized from ethanol. **2a**, yield 78 %; mp 180-182°C, **2b**, yield 80 %; mp 185-187°C; **3a**, yield 75 %; mp 210-211°C, **3b**, yield 64 %; mp 201-203°C. All data are identical with the reference manuscript. Nano-chitosan and chitosan encapsulated triazole derivatives (Ch-**2b**, Ch-**3a**, and Ch-**3b**) NPs were prepared using ionic gelation method [27]. Chitosan powder 0.5 g was

dissolved in 100 ml distilled water containing 2 ml acetic acid under continuous stirring. After complete dissolution, 0.05 g triazole derivatives (compounds **2a**, **3a**, and **3b**) were dissolved in 10 ml dimethyl sulfoxide (DMSO). The solution was added dropwise to chitosan solution under stirring for about 15 min. Sodium tripolyphosphate (0.33 g) was dissolved in 50 ml distilled water and then introduced to chitosan solution under stirring for 30 min. During the addition of TPP; the solution turned out to be turbid. It indicates the formation of encapsulated nano-chitosan. After the complete addition process; the nanoparticles dispersion remained under stirring for one more hour. Then, an amount of suspended solution was kept for analysis and characterization. The suspension was centrifuged at about 6000 rpm for 10 min. This step was followed by a freeze-drying process or lyophilization for 24 h. A blank sample of nano-chitosan was prepared using the same sequence but in the absence of triazole derivatives.

2.3. Synthesis of triazole encapsulated chitosan/selenium nanoparticles

The same procedure was repeated for synthesizing the encapsulated triazole derivatives/selenium nanoparticles, in the presence of selenous acid. The latter was added dropwise onto chitosan solution containing triazole derivatives under stirring at about 70°C for 1 h. TPP was added onto the obtained mixture for nano-chitosan encapsulation with continuing the same steps.

2.4. Characterization of the synthesized nanoparticles

To assess the reactive functional groups of the encapsulated nano-chitosan; Fourier transform infrared (FTIR) analysis was used within the range (400 - 4000 cm⁻¹) using Nicolet Avatar FTIR 370 CSI. The particle size and shape of nanoparticles were assessed using a transmission electron microscope (HR-TEM, JEOL- JEM-2100). The diluted nanoparticles suspension was sonicated for an hour. Then, one or two drops were dropped onto the testing grid and left for drying prior investigation. The particle size and/or zeta potential of the nano-capsules can be assessed by using Dynamic Light Scattering (DLS) technique. A Zetasizer instrument (Nano-ZS, Malvern Instruments Ltd., Zetasizer Ver, 704, UK) was employed to determine the particle size. The diluted suspension of the synthesized nanoparticles was well sonicated to guarantee well dispersed nano-capsules in aqueous media. They were then investigated using DLS instrument. The thermal stability of the new synthesized nano-capsules was explored using a thermogravimetric analysis (TGA) TA Q500 instrument, at a heating rate 10 °C/ min. in nitrogen atmosphere.

2.5. Biological activity

2.5.1. Cells

Cell line: human colon cancer cell line (HCT116) was obtained from American Type Culture Collection (Rockville, Maryland, USA). They are maintained in the Ludwik Hirszfeld Institute of Immunology and Experimental Therapy (Wroclaw, Poland). Cells were cultured in Eagle medium (IET, Wroclaw, Poland). They were supplemented with 2 mM L-glutamine, 10% fetal bovine serum, 8 µg/mL of insulin and 1% MEM non-essential amino acid solution 100x (all from Sigma-Aldrich Chemie GmbH, Steinheim, Germany).

2.5.2. Compounds

Prior to usage, the compounds were dissolved in DMSO (stock solution 10 mg/ml) and culture medium (1:9) to the concentration of 1 mg/ml. Subsequently, they were diluted in a culture medium to reach the required concentrations. It ranges from 100 to 0.1 µg/ml. Only the compound 3a was tested in various concentrations from 10 to 0.01 µg/ml. using a small amount of the tested compound.

2.5.3. An in vitro anti-proliferative assay

The cells were plated in 96-well plates (Sarstedt, Germany) at density of 1×10^4 cells per well for 24 h, before adding the tested compounds. The assay was implemented after being exposed to various concentrations of the investigated compounds for 72 h. The in vitro cytotoxic effect of all compounds was examined using the SRB assay.

2.5.4. Cytotoxic test SRB

The details of this technique were described by Skehan et al [28]. The cells were attached to the bottom of plastic wells by fixing them with cold 50% TCA (trichloroacetic acid, Sigma-Aldrich Chemie GmbH, Steinheim, Germany) on the top of the culture medium in each well. The plates were incubated at 4°C for 1 h. Then, they were washed five times with tap water. The cellular material fixed with TCA was stained with 0.4% sulphorhodamine B (SRB, Sigma-Aldrich Chemie GmbH, Steinheim, Germany). It was dissolved in 1% acetic acid (POCH, Gliwice, Poland) for 30 min. Unbound dye was removed by rinsing (5 times) in 1% acetic acid. The protein-bound dye was extracted with 10 mM buffered Tris base (POCH, microplate reader (BioTek Instruments USA). The cells were observed for morphological changes using Nikon TMS Inverted Microscope (New York- USA). Gliwice, Poland) for determining the optical density ($\lambda = 540$ nm) in Synergy H4 multi-mode. The relationship between surviving fraction and drug concentration was plotted to get the survival curve for each cell line after the specified time. The required concentration for 50% inhibition of cell viability (IC_{50})

was calculated. The results are represented in Table 1. They were compared to the antiproliferative effects of the reference control doxorubicin [29].

2.5.5. Statistical analysis

The results are reported as mean \pm standard deviation (S.D.) at least 3 times/experiment.

3. Results and discussion

Heterocyclic compounds are considered as major components in some chemical therapeutics. Thereafter, it is recommended to reduce the use of chemicals as much as possible to synthesize the targeted heterocyclic compounds. Nucleosides contribute in different pharmacological and biological applications. They exhibit antiviral, anticancer and antimicrobial activities [11]. The acyclic C-nucleosides 2a-d and Schiff base derivatives 3a,b of triazolopyrimidine were obtained in satisfactory yields (62-68%), **Scheme 1** [5].

Fig. 1 demonstrates the chemical structures of the prepared heterocyclic compounds investigated in this work. **2a**: 7-((Glucosylidene))amino)-8-methyl-5-(5-methylfuran-2-yl)pyrimido[5,4-*e*][1,2,4]triazolo[1,5-*a*]pyrimidin-6(7H)-one.

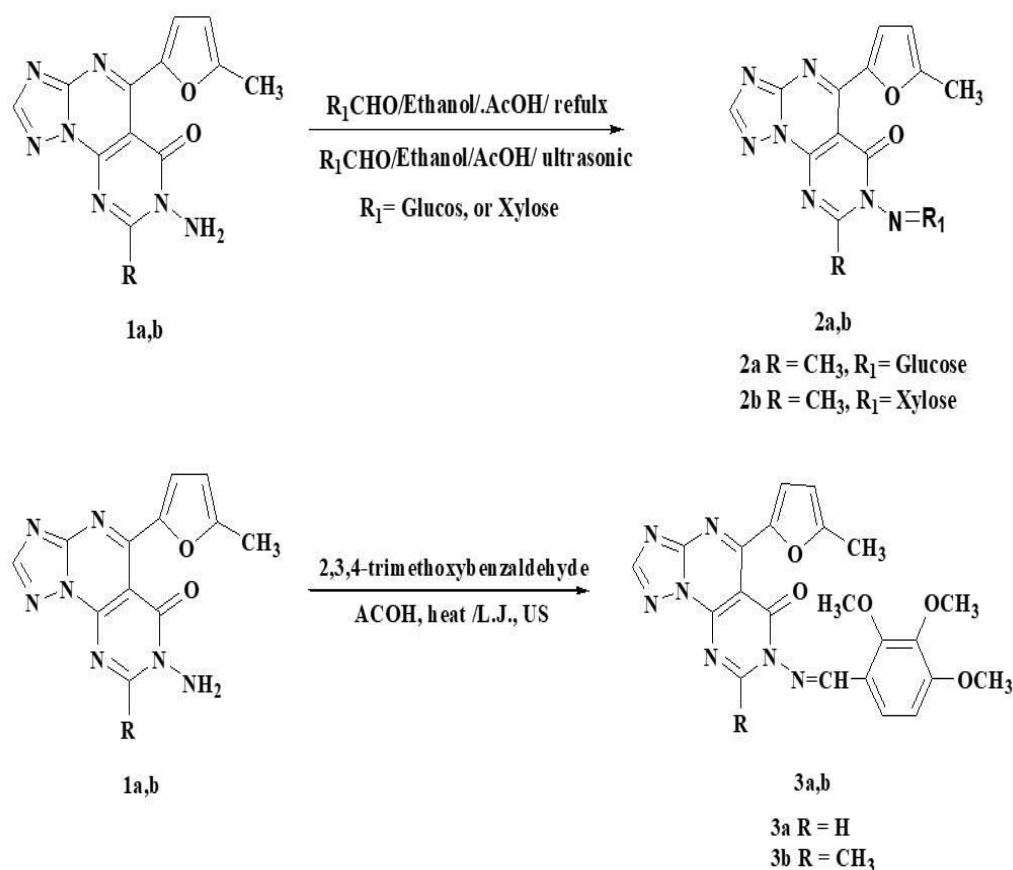
2b: 7-((Xylosylidene)amino))-8-methyl-5-(5-methylfuran-2-yl)-pyrimido[5,4-*e*][1,2,4]triazolo[1,5-*a*]pyrimidin-6(7H)-one.

3a: 5-(5-methylfuran-2-yl)-7-((2,3,4-trimethoxybenzylidene)-amino)pyrimido[5,4-*e*][1,2,4]triazolo[1,5-*a*]pyrimidin-6(7H)-one.

3b: 8-Methyl-5-(5-methylfuran-2-yl)-7-((2,3,4-trimethoxybenzylidene)amino)-pyrimido[5,4-*e*][1,2,4]triazolo[1,5-*a*]pyrimidin-6-one.

The synthesized nano-chitosan encapsulated triazole derivative with and without selenium nanoparticles were characterized using various techniques comprising FTIR, TEM, DLS and TGA analyses as follows:

FTIR spectra of chitosan encapsulated triazole **3a** and triazole **3b** with selenium nanoparticles are illustrated in Figure 2. The nano-chitosan showed well characterized peaks at 1869 and 2964 cm^{-1} referring to C-H and C-H₂ stretching bands. The broad band at 3220 cm^{-1} revealed the combination stretching of OH and NH₂ groups. Meanwhile, the band at 1623 cm^{-1} is assigned to CO of amide groups of un-hydrolyzed chitin part in chitosan. The peaks at 1530 and 1064 cm^{-1} revealed the presence of N-H bending and C-N stretching. The nano-capsule containing selenium nanoparticles showed a characteristic IR spectrum with major peaks indicating chitosan. It demonstrates the remaining of N-acetyl groups with slight shifting in some peaks from 1623 cm^{-1} to 1638 cm^{-1} .



Scheme 1. The synthesis of acyclic C-nucleosides 2a,b and Schiff base derivatives 3a,b of triazolopyrimidine.

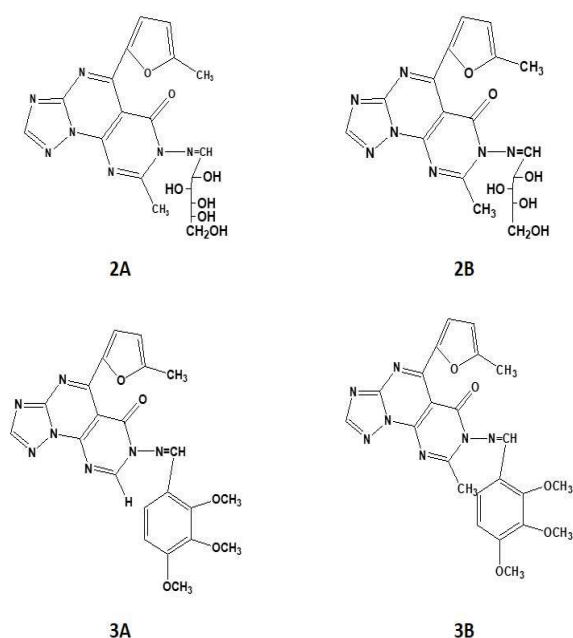


Fig. 1. The chemical structures of the synthesized heterocyclic compounds **2a**, **2b**, **3a** and **3b**.

The broad characteristic band at 3220 cm^{-1} shifted to 3226 cm^{-1} . A new peak at 3386 cm^{-1} of OH groups was

noticed. The presence of selenium nanoparticles may be observed at 703 cm^{-1} .

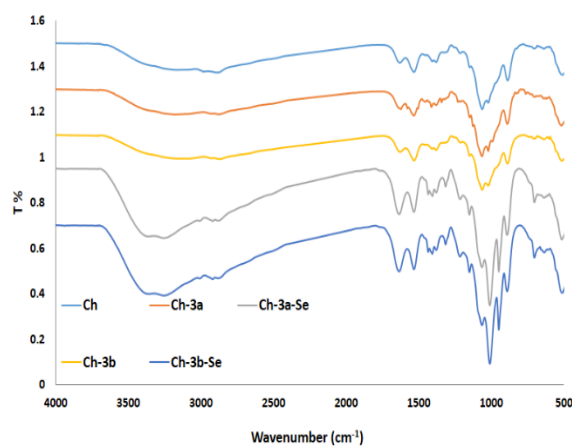


Fig. 2. FTIR of Ch, Ch-3a, Ch-3a-Se, Ch-3b and Ch-3b-Se.

The size and shape of the synthesized nanoparticles were evaluated using transmission electron microscope (TEM) as shown in Fig. 3. The blank nano-chitosan (Fig. 3a) has a semi-spherical shape with a nodal structure. They possess an average size of 50 to 80 nm. Fig. 3 (b-d) showed the synthesized chitosan nanoparticles encapsulated

triazole derivatives (**2b**, **3a** and **3b**). The figure showed that the semi-spherical shape of these nanoparticles exhibit a slight increase in the size. Moreover, the appearance of some aggregations in the nanoparticles may be referred to the relative larger size and hydrogen bonding between the particles [5]. The dark spots in the figure indicate that the triazole derivatives spread within and outside the chitosan nanoparticles. The encapsulated particles may be released out from the nano-capsule due to the presence of the nanoparticle in the solution. It stimulates the encapsulated compound to be released. It should be centrifuged immediately after nanoparticles synthesis or up to 30 min. later. The prepared nano-capsules remained suspended in the solution for TEM characterization.

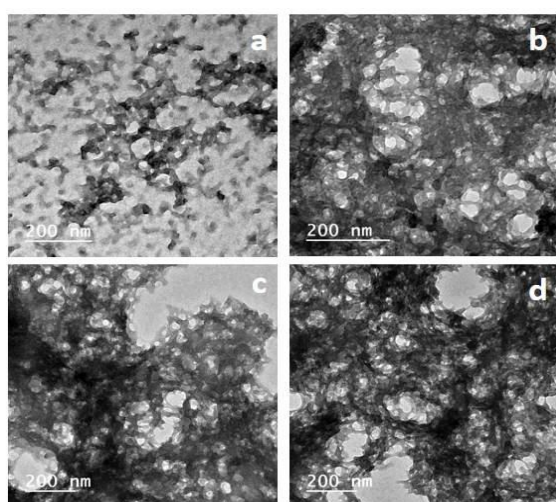


Fig. 3. TEM of (a) Ch, (b) Ch-**2b**, (c) Ch-**3a** and (d) Ch-**3b**.

The particle size can be evaluated using dynamic light scattering measurements. It depends on measuring the scattered beam occurring due to the Brownian motion of suspended nanoparticles in the solution. Fig. 4 (a-c) showed the average particle size of chitosan nanoparticles encapsulated triazole compound with selenium nanoparticles. It is clearly seen that the size of nanoparticles were 77, 197, and 292 nm for Ch-**2b**-Se, Ch-**3b**-Se and Ch-**3a**-Se, respectively. The variation in the particle size may be due to the relative affinity or polarity and solubility of the different compound with the entire vehicle. The larger particle size obtained from DLS rather than that obtained by TEM measurement may be noticed. This remark can be correlated to delivering an image for definite area for measurement via TEM whereas DLS gives an overall observation for the nanoparticles and their agglomeration. In addition, DLS measurement provides a hydrodynamic radius of nanoparticles (hydrated and swollen particles) in aqueous solution. On the other hand, TEM provides the diameter of dried nanoparticles.

Zeta potential of the synthesized nanoparticles are displayed in Fig. 5. Zeta potential measures the surface charges of the nanoparticles which are positively charged. This is due to the cationic nature of the amine groups in the protonated form resulted from the acidic solvent medium for chitosan [27]. Upon encapsulating triazole derivatives, the zeta potential showed different values of 29.2, 35.6 and 27 mV for Ch-**2b**, Ch-**3b** and Ch-**3a**, respectively. The thermal stability of the synthesized nanoparticles was assessed via using thermogravimetric analysis (TGA). Nano-chitosan showed two degradation steps as shown in Fig. 6. The first one ranged from 54 to 130°C representing the adsorbed moisture. The second degradation step ranged from 220 to 390°C. It is assigned to the thermal degradation of the main backbone of chitosan chains [4,26]. The thermogram of the chitosan encapsulated triazole **3b** showed similar behavior with an enhanced thermal stability to that of sole chitosan. The remaining weight percent after the main chain degradation was 56 % for triazole encapsulated nano-chitosan. Moreover, the pure nano-chitosan showed a 47% weight loss. The thermal degradation of the nano-capsule incorporated selenium nanoparticles was much stable than the other ones without selenium nanoparticles. The first degradation step showed a 4 % weight loss at 130°C. It represented less water content. It reached 11% for chitosan and chitosan triazole nano-capsule. The second weigh loss of selenium incorporated nanoparticles reached about 15 % after 320°C. It represents a higher thermal stability for capsules loaded with inorganic metal nanoparticles.

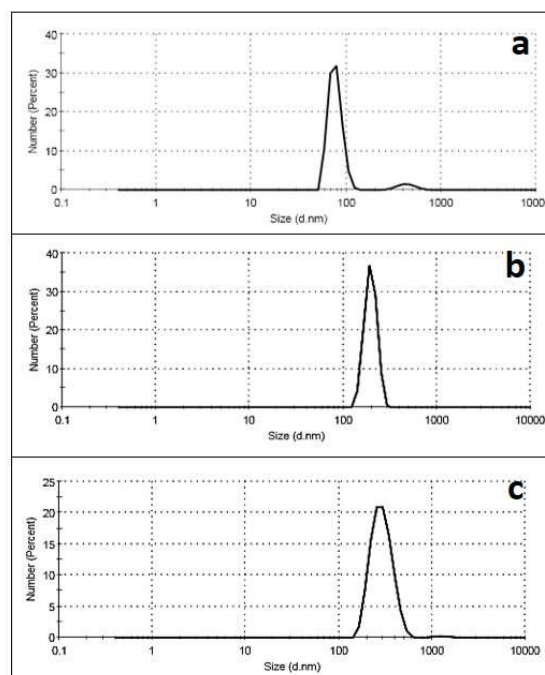


Fig. 4. Particle size of (a) Ch-**2b**-Se, (b) Ch-**3b**-Se and (c) Ch-**3a**-Se (77, 197, and 292 nm).

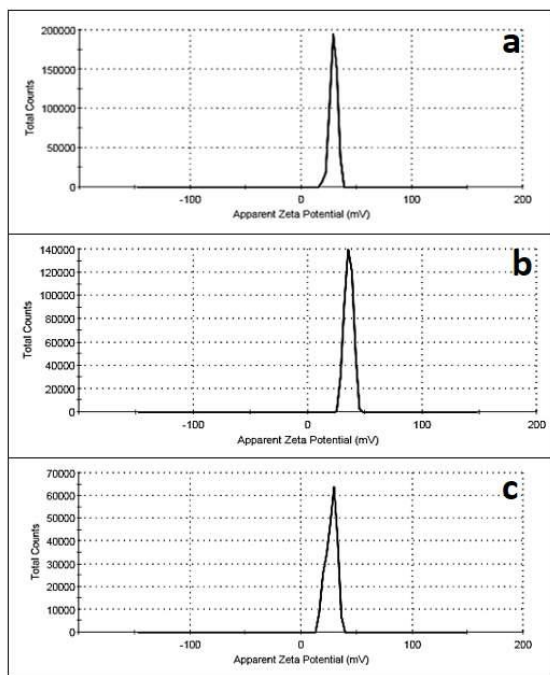


Fig. 5. Zeta Potential of (a) Ch-**2b**-Se, (b) Ch-**3b**-Se and (c) Ch-**3a**-Se (29.2, 35.6, and 27 mV).

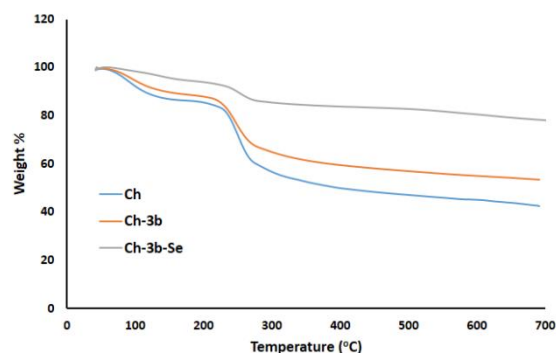


Fig. 6. TGA of Ch, Ch-**3b** and Ch-**3b**-Se.

The in vitro cytotoxicity of the synthesized nanocapsules was investigated towards human colon cancer cell line (HCT116) via standard established assays. The antiproliferative activities were expressed by median growth inhibitory concentration (IC_{50}). As shown in table 1, the in vitro antiproliferative activity towards human colon cancer cell line (HCT116) was evaluated using SRB assay, in comparison with doxorubicin as reference drug. The data indicated that all compounds showed a variable activity against human colon cancer cell line (HCT116). The tumor cell line showed normal growth in our culture system. DMSO did not seem to have any noticeable effect on cellular growth. A gradual decrease in the viability of cancer cells was observed with increasing concentration of the tested compounds, in a dose-dependent inhibitory effect. Evaluating the antitumor effect of the tested compounds towards human colon cancer (HCT116) cells revealed that chitosan alone had moderate effect on these cancer cells with IC_{50}

value $32.09 \pm 2.01 \mu\text{g/ml}$. Meanwhile, the compound **3b**-Se was found to be the highest potent derivative followed by **3a**-Se in comparison to doxorubicin the standard anticancer drug. It displayed an IC_{50} value of $5.21 \pm 0.04 \mu\text{g/ml}$ and $7.32 \pm 0.06 \mu\text{g/ml}$ versus $4.53 \pm 0.08 \mu\text{g/ml}$ for doxorubicin. Moreover, compounds **2b**, **3b** and **3a** without SE showed good activity with IC_{50} values. They are IC_{50} : 21.08 ± 0.7 , 15.72 ± 0.4 and $18.3 \pm 0.6 \mu\text{g/ml}$ respectively versus $4.53 \pm 0.08 \mu\text{g/ml}$ for doxorubicin.

Figure 7. demonstrates the antiproliferative potency of triazoles loaded onto chitosan with selenium (**3a**-Se and **3b**-Se) and without selenium (**2b**, **3a** and **3b**) in comparison to chitosan alone towards human colon cancer cell line (HCT116). As shown in the figure, compound **3b**-Se was found to be the highest potent derivative followed by **3a**-Se. Furthermore, compounds **2b**, **3b** and **3a** without selenium showed good activity. This observation was supported by determining the IC_{50} values of these compounds as indicated in table 1. The difference in the cytotoxicity of these compounds can be attributed to variations in their interaction mechanism owing to the presence of different biomolecules on their surfaces.

Table 1: In vitro cytotoxic activity of the newly synthesized compounds towards human colon cancer cell line (HCT116) is expressed as IC_{50} values.

Compounds	Colon (HCT 116) IC_{50} [$\mu\text{g/ml}$]
Ch-2b	21.08 ± 0.7
Ch-3b	15.72 ± 0.4
Ch-3a	18.3 ± 0.6
Ch-3b-Se	5.21 ± 0.04
Ch-3a-Se	7.32 ± 0.06
Ch	32.09 ± 2.01
Doxorubicin	4.53 ± 0.08
DMSO	N.A.

Data were expressed as Mean \pm SD of three independent experiments. N.A.: No activity

A further investigation for the mechanism of cytotoxicity was carried out via analyzing the morphological changes in the treated cells. As indicated in Fig. 7, a change was observed in the morphology of the HCT116 cells treated with compounds **2b**, **3a** and **3b** without selenium in comparison with that of the untreated cells. The cells were found to be detached from the surface and had lost their original morphology. The intensity increased upon treatment with compounds **3a**-Se and **3b**-Se as the cell viability decreased. The mechanism of the cytotoxicity of selenium nanoparticles has been described in many reports [30–32].

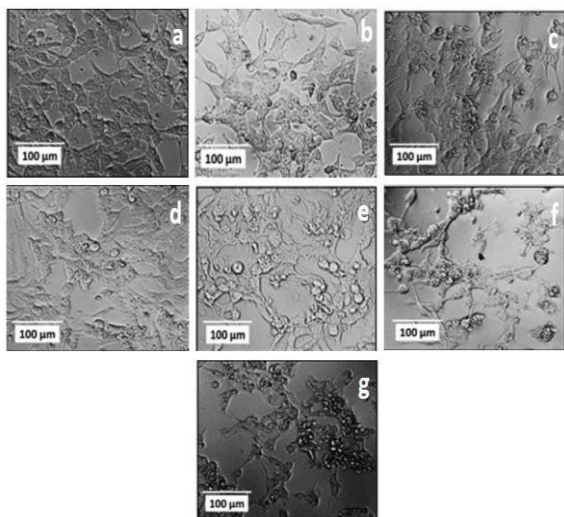


Fig. 7. Cytotoxicity of triazole derivatives loaded on chitosan with selenium (**3a-Se** and **3b-Se**) and without selenium (**2b**, **3a** and **3b**) in comparison to chitosan alone towards human colon cancer cell line (HCT116): (a) Untreated (b) Chitosan (c) **2b** (d) **3b** (e) **3a** (f) **3b-Se** (g) **3a-Se**.

4. Conclusions

The synthesis of triazole derivative encapsulated nano-chitosan with and without selenium nanoparticles (SeNPs) was successfully performed using ionic gelation method. Various techniques were employed to investigate the synthesized nanoparticles. They confirmed the formation of nanoparticles with spherical shape and good thermal stability. The efficacy of the synthesized triazole derivative encapsulated nano-chitosan with and without selenium nanoparticles towards human colon cancer cell line (HCT116) was investigated. The assessment of their cytotoxicity demonstrated their concentration-dependence through in vitro anti-proliferative activity in this cancer cell line. In conclusion, the tested compounds exerted an anti-proliferative activity on human colon cancer cell line (HCT116) through reducing cell proliferation. It resulted in significant growth inhibitory effect. The compounds Ch-**2b**, Ch-**3b** and Ch-**3a** showed good cytotoxicity and growth inhibitor activity on colon cancer cell line with IC₅₀ values near to the standard drug. Meanwhile, the compounds Ch-**3b-Se** and Ch-**3a-Se** were found to be the most potent on this type of cell line. This study has pointed out to the need of right selection in green organic compounds and methodologies for the synthesis of selenium nanoparticles for different purposes with respect to the environment and human health.

Acknowledgments

The authors acknowledge National Research Centre (NRC) - Egypt; for funding this work through: Project no.12020205.

Conflict of Interests

The authors declare no conflict of interest.

References

1. Bray, F.; Ferlay, J.; Soerjomataram, I.; Siegel, R.L.; Torre, L.A.; Jemal, A. Global Cancer Statistics, GLOBOCAN Estimates of Incidence and Mortality Worldwide for 36 Cancers in 185 Countries. *CA. Cancer J. Clin.* 2018, 68, 394–424 (2018), doi:10.3322/caac.21492.
2. Lee, M.M.L.; Chan, B.D.; Wong, W.Y.; Leung, T.W.; Qu, Z.; Huang, J.; Zhu, L.; Lee, C.S.; Chen, S.; Tai, W.C.S. Synthesis and Evaluation of Novel Anticancer Compounds Derived from the Natural Product Brevilin A. *ACS omega*, 5, 14586–14596 (2020), doi:10.1021/ACSOMEGA.0C01276.
3. Spyridopoulou, K.; Aindelis, G.; Pappa, A.; Chlichlia, K. Anticancer Activity of Biogenic Selenium Nanoparticles: Apoptotic and Immunogenic Cell Death Markers in Colon Cancer Cells. *Cancers*, Vol. 13, Page 5335 2021, 13, 5335 (2021), doi:10.3390/CANCERS13215335.
4. Mazarei, M.; Mohammadi Arvejeh, P.; Mozafari, M.R.; Khosravian, P.; Ghasemi, S. Anticancer Potential of Temozolomide-Loaded Eudragit-Chitosan Coated Selenium Nanoparticles: In Vitro Evaluation of Cytotoxicity, Apoptosis and Gene Regulation. *Nanomater.*, Vol. 11, Page 1704 2021, 11, 1704 (2021), doi:10.3390/NANO11071704.
5. Khattab, R.R.; Swelam, S.A.; Khalil, A.M.; Abdelhamid, A.E.; Soliman, A.M.; El-Sayed, A.A. Novel Sono-Synthesized Triazole Derivatives Conjugated with Selenium Nanoparticles for Cancer Treatment. *Egypt. J. Chem.*, 64, 4675–4688 (2021), doi:10.21608/EJCHEM.2021.81154.4018.
6. Bilek, O.; Fohlerova, Z.; Hubalek, J. Enhanced Antibacterial and Anticancer Properties of Se-NPs Decorated TiO₂ Nanotube Film. *PLoS One*, 14 (2019), doi:10.1371/JOURNAL.PONE.0214066.
7. El-Ghazaly, M.A.; Fadel, N.; Rashed, E.; El-Batal, A.; Kenawy, S.A. Anti-Inflammatory Effect of Selenium Nanoparticles on the Inflammation Induced in Irradiated Rats. *Can. J. Physiol. Pharmacol.*, 95, 101–110 (2017), doi:10.1139/CJPP-2016-0183/ASSET/IMAGES/LARGE/CJPP-2016-0183F5.JPEG.
8. Kondaparthi, P.; Flora, S.; Naqvi, S. Selenium Nanoparticles: An Insight on Its Pro-Oxidant and Antioxidant Properties. *Front. Nanosci. Nanotechnol.*, 6 (2019), doi:10.15761/FNN.1000189.
9. El-Sayed, A.A.; Abu-Bakr, S.M.; Swelam,

- S.A.; Khaireldin, N.Y.; Shoueir, K.R.; Khalil, A.M. Applying Nanotechnology in the Synthesis of Benzimidazole Derivatives: A Pharmacological Approach. *Review*, 12, 992–1005 (2022), doi:10.33263/BRIAC121.9921005.
10. Abu-Bakr, S.M.; Khidre, M.D.; Omar, M.A.; Swelam, S.A.; Awad, H.M. Synthesis of Furo[3,2-g]Chromones under Microwave Irradiation and Their Antitumor Activity Evaluation. *J. Heterocycl. Chem.*, 57, 731–743 (2020), doi:10.1002/JHET.3813.
 11. Khattab, R.R.; Hassan, A.A.; Kutkat, O.M.; Abuzeid, K.M.; Hassan, N.A. Synthesis and Antiviral Activity of Novel Thieno[2,3-d]Pyrimidine Hydrazones and Their C-Nucleosides. *Russ. J. Gen. Chem.*, 89, 1707–1717 (2019), doi:10.1134/S1070363219080267.
 12. Eya'ane Meva, F.; Prior, T.J.; Evans, D.J.; Shah, S.; Tamngwa, C.F.; Belengue, H.G.L.; Mang, R.E.; Munro, J.; Qahash, T.; Llinás, M. Anti-Inflammation and Antimalarial Profile of 5-Pyridin-2-yl-1H-[1,2,4]Triazole-3-Carboxylic Acid Ethyl Ester as a Low Molecular Intermediate for Hybrid Drug Synthesis. *Res. Chem. Intermed.*, 48, 885–898 (2022), doi:10.1007/S11164-021-04607-3/FIGURES/9.
 13. Kaushik, C.P.; Chahal, M. Synthesis, Antimalarial and Antioxidant Activity of Coumarin Appended 1,4-Disubstituted 1,2,3-Triazoles. *Monatshefte für Chemie*, 152, 1001–1012 (2021), doi:10.1007/S00706-021-02821-8/TABLES/2.
 14. Groaz, E.; De Jonghe, S. Overview of Biologically Active Nucleoside Phosphonates. *Front. Chem.*, 8, 1212 (2021), doi:10.3389/FCHEM.2020.616863/BIBTEX.
 15. De Jonghe, S.; Herdewijn, P. An Overview of Marketed Nucleoside and Nucleotide Analogs. *Curr. Protoc.*, 2, e376 (2022), doi:10.1002/CPZ1.376.
 16. Singh, S. Nanomedicine-Nanoscale Drugs and Delivery Systems. *J. Nanosci. Nanotechnol.*, 10, 7906–7918 (2010), doi:10.1166/JNN.2010.3617.
 17. Stewart, B.W.; Wild, C.P. The Global and Regional Burden of Cancer. In *World Cancer Report 2014*; Stewart, B. W., Wild, C.P., Ed.; 1st ed.; International Agency for Research on Cancer: Lyon, (2014); ISBN 9789283204435.
 18. Torre, L.A.; Bray, F.; Siegel, R.L.; Ferlay, J.; Lortet-Tieulent, J.; Jemal, A. Global Cancer Statistics, 2012. *CA. Cancer J. Clin.*, 65, 87–108 (2015), doi:10.3322/CAAC.21262.
 19. Afzal, B.; Fatma, T. Selenium Nanoparticles: Green Synthesis and Exploitation. *Emerg. Technol. Nanoparticle Manuf.*, 473–484 (2021), doi:10.1007/978-3-030-50703-9_22.
 20. Shi, X.D.; Tian, Y.Q.; Wu, J.L.; Wang, S.Y. Synthesis, Characterization, and Biological Activity of Selenium Nanoparticles Conjugated with Polysaccharides. *Crit. Rev. Food Sci. Nutr.*, 61, 2225–2236 (2021), doi:10.1080/10408398.2020.1774497.
 21. Aliabadi, H.M.; Lavasanifar, A. Polymeric Micelles for Drug Delivery. *Expert Opin. Drug Deliv.*, 3, 139–162 (2005), doi:10.1517/17425247.3.1.139.
 22. Pinto Reis, C.; Neufeld, R.J.; Ribeiro, A.J.; Veiga, F. Nanoencapsulation I. Methods for Preparation of Drug-Loaded Polymeric Nanoparticles. *Nanomedicine Nanotechnology, Biol. Med.*, 2, 8–21 (2006), doi:10.1016/J.NANO.2005.12.003.
 23. Dash, T.K.; Konkimalla, V.B. Poly-ε-Caprolactone Based Formulations for Drug Delivery and Tissue Engineering: A Review. *J. Control. Release*, 158, 15–33 (2012), doi:10.1016/J.JCONREL.2011.09.064.
 24. Kumari, A.; Yadav, S.K.; Yadav, S.C. Biodegradable Polymeric Nanoparticles Based Drug Delivery Systems. *Colloids Surf. B. Biointerfaces*, 75, 1–18 (2010), doi:10.1016/J.COLSURFB.2009.09.001.
 25. Xie, Z.; Shen, J.; Sun, H.; Li, J.; Wang, X. Polymer-Based Hydrogels with Local Drug Release for Cancer Immunotherapy. *Biomed. Pharmacother.*, 137, 111333 (2021), doi:10.1016/J.BIOPHA.2021.111333.
 26. Kamath, P.R.; Sunil, D. Nano-Chitosan Particles in Anticancer Drug Delivery: An Up-to-Date Review. *Mini Rev. Med. Chem.*, 17 (2017), doi:10.2174/1389557517666170228105731.
 27. Fan, W.; Yan, W.; Xu, Z.; Ni, H. Formation Mechanism of Monodisperse, Low Molecular Weight Chitosan Nanoparticles by Ionic Gelation Technique. *Colloids Surf. B. Biointerfaces*, 90, 21–27 (2012), doi:10.1016/J.COLSURFB.2011.09.042.
 28. Skehan, P.; Storeng, R.; Scudiero, D.; Monks, A.; McMahon, J.; Vistica, D.; Warren, J.T.; Bokesch, H.; Kenney, S.; Boyd, M.R. New Colorimetric Cytotoxicity Assay for Anticancer-Drug Screening. *JNCI J. Natl. Cancer Inst.*, 82, 1107–1112 (1990), doi:10.1093/JNCI/82.13.1107.
 29. Wander, D.P.A.; Van Der Zanden, S.Y.; Vriends, M.B.L.; Van Veen, B.C.; Vlaming, J.G.C.; Bruyning, T.; Hansen, T.; Van Der Marel, G.A.; Overkleeft, H.S.; Neeffjes, J.J.C.; et al. Synthetic (N, N-Dimethyl)Doxorubicin Glycosyl Diastereomers to Dissect Modes of Action of Anthracycline Anticancer Drugs. *J. Org. Chem.*, 86, 5757–5770 (2021), doi:10.1021/ACS.JOC.1C00220.

30. Varlamova, E.G.; Goltyaev, M. V.; Mal'tseva, V.N.; Turovsky, E.A.; Sarimov, R.M.; Simakin, A. V.; Gudkov, S. V. Mechanisms of the Cytotoxic Effect of Selenium Nanoparticles in Different Human Cancer Cell Lines. *Int. J. Mol. Sci.*, 22 (2021), doi:10.3390/IJMS22157798.
31. Alkudhayri, A.A.; Wahab, R.; Siddiqui, M.A.; Ahmad, J. Selenium Nanoparticles Induce Cytotoxicity and Apoptosis in Human Breast Cancer (MCF-7) and Liver (HepG2) Cell Lines. *Nanosci. Nanotechnol. Lett.*, 12, 324–330 (2020), doi:10.1166/nnl.2020.3115.
32. Shahabadi, N.; Zendehehsh, S.; Khademi, F. Selenium Nanoparticles: Synthesis, in-Vitro Cytotoxicity, Antioxidant Activity and Interaction Studies with Ct-DNA and HSA, HHb and Cyt c Serum Proteins. *Biotechnol. Reports*, 30, e00615 (2021), doi:10.1016/J.BTRE.2021.E00615.